

Transient thermal wave techniques for the evaluation of surface coatings

To cite this article: S K Lau *et al* 1991 *J. Phys. D: Appl. Phys.* **24** 428

View the [article online](#) for updates and enhancements.

Related content

- [The accuracy of thermal wave interferometry for the evaluation of thermophysical properties of plasma-sprayed coatings](#)
A C Bento and D P Almond
- [Thermal-wave interferometry](#)
A Bendada
- [Analysis of multifunctional oxycarbide and oxynitride thin films by modulated IR radiometry](#)
J Gibkes, F Vaz, A C Fernandes *et al.*

Recent citations

- [Experimentally validated defect depth estimation using artificial neural network in pulsed thermography](#)
Numan Saeed *et al*
- [Utilization of linearization methods for measuring of thermal properties of materials](#)
Ivo Spicka *et al*
- [Nanoscale thermal diffusion during the laser interference ablation using femto-, pico-, and nanosecond pulses in silicon](#)
Mindaugas Gedvilas *et al*



IOP | ebooks™

Bringing together innovative digital publishing with leading authors from the global scientific community.

Start exploring the collection—download the first chapter of every title for free.

Transient thermal wave techniques for the evaluation of surface coatings

S K Lau, D P Almond and P M Patel

School of Materials Science, University of Bath, Claverton Down, Bath BA2 7AY, UK

Received 26 April 1990, in final form 26 November 1990

Abstract. A thermal wave interference model is developed to analyse the response of coatings to pulsed and stepped heating. The influence of the relative thermal properties of coating and substrate and the possibility of coating translucency are included in the analysis. The potential of transient techniques for the measurement of coating thickness is demonstrated and compared with the continuous wave technique. Experimental results obtained from plasma sprayed zirconia coatings are presented and compared with theoretical predictions.

1. Introduction

The characteristics of thermal wave techniques in the testing of surface coatings and the characterization of sub-surface structural defects has been extensively reported [1–8]. The techniques are attractive because they are non-destructive and non-contacting and because they can provide information about certain types of coatings which cannot be readily tested by established techniques.

Many different ways of generating thermal waves at the sample surface are possible and many different techniques may be adopted to detect the thermal wave interference effects that occur in a coating. A modulated laser beam is the most commonly used means of generating thermal waves, which are often detected by a photo-acoustic cell or an infrared detector. The periodically modulated heating (known as the chopped continuous wave or CW) technique has been investigated in some detail [1–3], and experimental results have shown good consistency with the theory of thermal wave interferometry. However, less work has been done on the analysis of transient thermal wave techniques, though Cielo *et al* [5–7] have shown that the general features are understood. The purpose of this paper is to demonstrate that the observations made using these transient techniques may be attributed to thermal wave interference. In addition, we show how useful information may be extracted from these observations. As an understanding of the phenomenon of thermal wave propagation and thermal wave interferometry is essential, this is described first in some detail in the following section.

2. Theory

2.1. Thermal wave interferometry

Heat flows periodically in a sample as a thermal wave when its surface is subjected to a periodically

modulated heat source, e.g. by photothermal excitation or other means. The nature of thermal propagation results in the thermal wave being heavily damped. For a one-dimensional thermal wave propagating in the positive x direction, this temperature variation may be expressed in complex form as ([10] pp 64–9)

$$T(x, t) = T_0 \exp(-x/\mu) \exp[j(\omega t - x/\mu)] \quad (1)$$

where T_0 is the initial change in temperature produced by the source, $\omega (=2\pi f)$ is the angular modulation frequency, and $j = (-1)^{1/2}$. In a distance μ , known as the thermal diffusion length, the wave is attenuated by a factor of $1/e$ and its phase changes by 57 degrees. The diffusion length μ is determined by the angular frequency ω and the thermal diffusivity α of the sample:

$$\mu = (2\alpha/\omega)^{1/2} \quad (2)$$

Consider now the case of a coating of thickness L on a thermally thick substrate. Thermal waves will undergo reflection of scattering processes when they encounter regions or different thermal characteristics. The reflection coefficient Γ for a thermal wave, propagating in medium 1 (the coating), at an interface with medium 2 (the substrate), is given by [9]

$$\Gamma = (1 - b)/(1 + b) \quad b = \left(\frac{(\rho ck)_2}{(\rho ck)_1} \right)^{1/2} \quad (3)$$

where ρ is the mass density, c is the specific heat capacity, and k is the thermal conductivity of the respective media. These reflected and incident thermal waves interfere with each other at the sample surface to produce a thermal interference phenomenon.

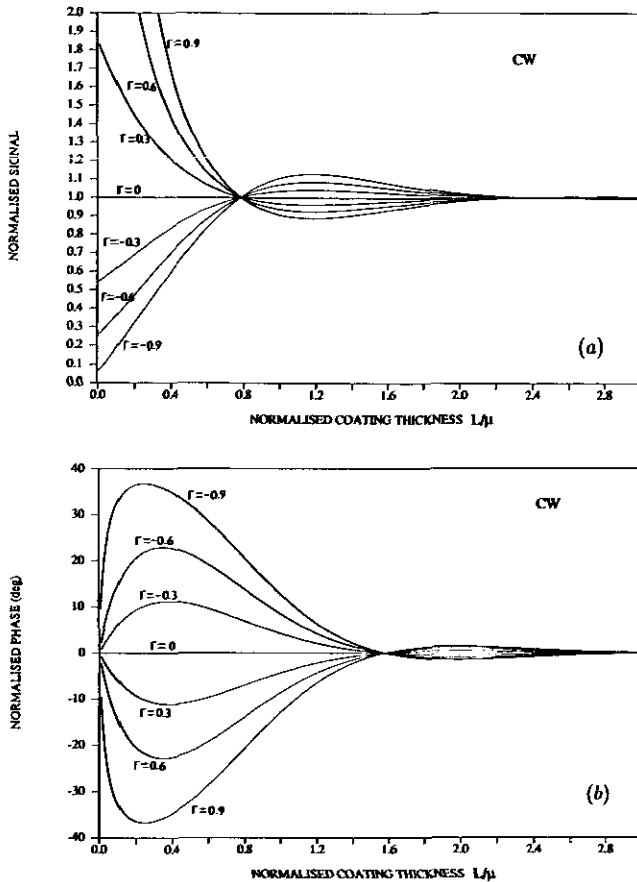


Figure 1. (a) Variation of the change in signal caused by thermal wave interference in CW modulation, plotted as a function of normalized coating thickness (L/μ) for different reflection coefficients Γ . (b) Variation of the change in phase angle caused by thermal wave interference in CW modulation, plotted as a function of normalized coating thickness (L/μ) for different reflection coefficients Γ .

Bennett and Patty [9] analysed this thermal wave interference to obtain a general expression for the resultant surface temperature in complex form:

$$T(j\omega) = \frac{(1-r)I_0}{2k\sigma} \left[\frac{1 + \Gamma \exp(-2\sigma L)}{1 - \Gamma \exp(-2\sigma L)} \right] \quad (4)$$

where I_0 is the flux density of the applied heat source per unit area, r is the surface reflection coefficient of the coating and σ is the complex thermal wave vector given by

$$\sigma = (1 + j)/\mu. \quad (5)$$

The coating material is assumed to be optically opaque to the excitation beam. The changes in thermal wave amplitude and phase, caused by interference, are shown in figures 1(a) and (b) respectively, plotted as a function of normalized coating thickness L/μ . As might be expected for interference phenomena, both thermal wave amplitude and phase angle vary with coating thickness. This variation, because of the heavily damped nature of the thermal wave, is confined to coatings whose thicknesses are comparable to the thermal diffusion length μ . Thus, as there is a means of

obtaining the appropriate diffusion length μ , thermal wave interference can be used to assess coating thickness. In the case of the periodically modulated heating technique this is achieved by selecting the appropriate modulation frequency ω , since $\mu = (2\alpha/\omega)^{1/2}$ (equation (2)).

Alternatively, we may adopt the non-periodic approach by exciting the sample surface with a single high energy laser pulse and observing the transient temperature variation in time. This is known as the 'flash' technique for measuring the thermal diffusivity of a thin sample by monitoring the surface temperature at its back face [10]. In flash excitation, a broad Fourier frequency spectrum of thermal waves is generated to propagate into the sample. These decay at different rates and have different wavelengths; both determined by μ (equation (2)). The energy distribution of such a laser pulse is spread through a broad band of frequencies. In contrast, a step-like pulse of very long duration has a higher energy distribution concentrated at lower frequencies. In either case, there will be a proportion of the excited waves of the appropriate frequencies such that their thermal diffusion lengths are comparable to or greater than the coating thickness. These will be reflected to the surface to produce interference effects. These two techniques are related via a direct integration and differentiation of the transient responses and vice versa.

We have derived the theoretical surface temperature expressions, using methods that are the transient analogue of those employed by Bennett and Patty, for the pulse excitation with very short duration, which may be represented by the Dirac delta function $\delta(t)$, and the long duration step-like excitation. Both are readily obtainable from straightforward Laplace inversions of equation (4). This produces the solution of the thermal diffusion equation for the surface temperature of a two-layer model. For a short pulse:

$$T(0, t) = \frac{I_0}{4(\pi\rho ckt)^{1/2}} \left[1 + 2 \sum_{n=1}^{n=\infty} \Gamma^n \exp[-n^2 L^2 / (\alpha t)] \right] \quad (6)$$

and for a step-like pulse:

$$T(0, t) = \frac{I_0(\alpha t)^{1/2}}{2k} \left[\pi^{-1/2} + 2 \sum_{n=1}^{n=\infty} \Gamma^n i \operatorname{erfc}[nL / (\alpha t)^{1/2}] \right] \quad (7)$$

where

$$i \operatorname{erfc}(x) = \pi^{-1/2} \exp(-x^2) - x(1 - \operatorname{erf}(x)) \quad (7b)$$

and $\operatorname{erf}(x)$ is the error function of x .

Here we assume the coating surface is highly absorbing to the excitation beam, i.e. $r = 0$, and is optically opaque. The summation term appearing in each expression accounts for the total thermal wave contribution of internal multiple reflections between the interface and the surface.

The changes in surface temperature of the two excitation modes are shown plotted logarithmically as a

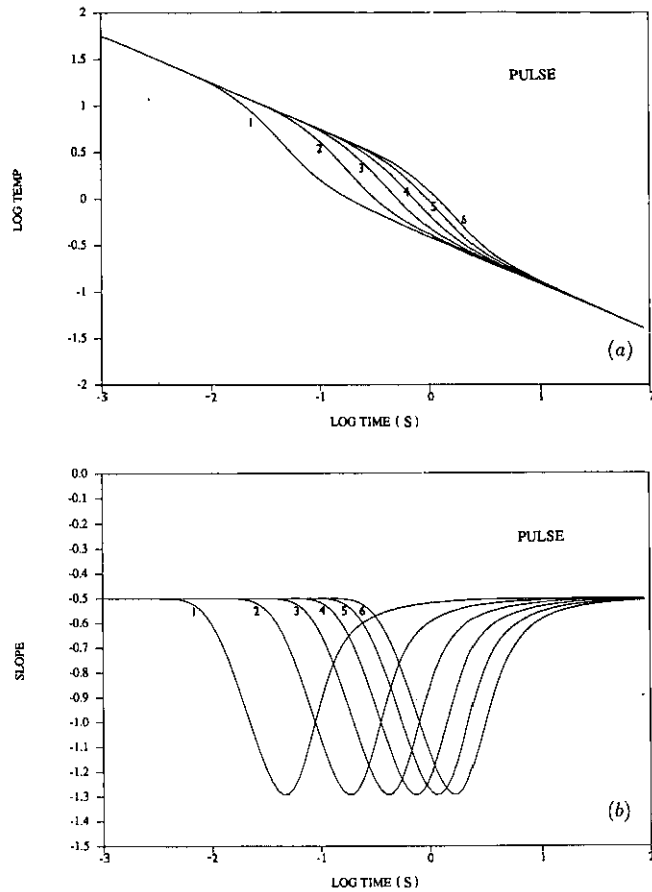


Figure 2. (a) Variation of surface temperature transients computed for pulse-heated opaque yttria-stabilized zirconia coatings on 316-stainless steel substrate. Heat flux $I_0 = 10000 \text{ W m}^{-2}$. Coating thicknesses are (1) 125, (2) 250, (3) 375, (4) 500, (5) 625 and (6) 750 μm . (b) Computed slope values of figure 2(a) for the pulsed heating of zirconia coatings of the same thicknesses as in figure 2(a).

function of time for different coating thicknesses in figures 2(a) and 3(a). In each case, the computations are for a plasma-sprayed yttria-stabilized zirconia coating, a thermal barrier coating of considerable current interest, on a 316-stainless steel substrate. The assumed mass densities, specific heat capacities and thermal conductivities for the zirconia coating were 5000 kg m^{-3} , $500 \text{ J kg}^{-1} \text{ K}^{-1}$ and $1 \text{ W m}^{-1} \text{ K}^{-1}$; while those of the steel substrate were 8230 kg m^{-3} , $470 \text{ J kg}^{-1} \text{ K}^{-1}$ and $14 \text{ W m}^{-1} \text{ K}^{-1}$ respectively. Figure 2(a) clearly shows that the initial thermal decay after the absorption of a Dirac-delta heating pulse of energy I_0 has a constant dimensionless logarithmic slope of $-\frac{1}{2}$, which corresponds to that of the thermal propagation in a homogeneous semi-infinite solid ([11] p 256):

$$T(x, t) = \frac{I_0}{4(\pi\rho ckt)^{1/2}} \exp[-x^2/(4\alpha t)] \quad (8)$$

which at the surface becomes,

$$T(0, t) = \frac{I_0}{4(\pi\rho ckt)^{1/2}}. \quad (9)$$

The interruption of the constant logarithmic thermal

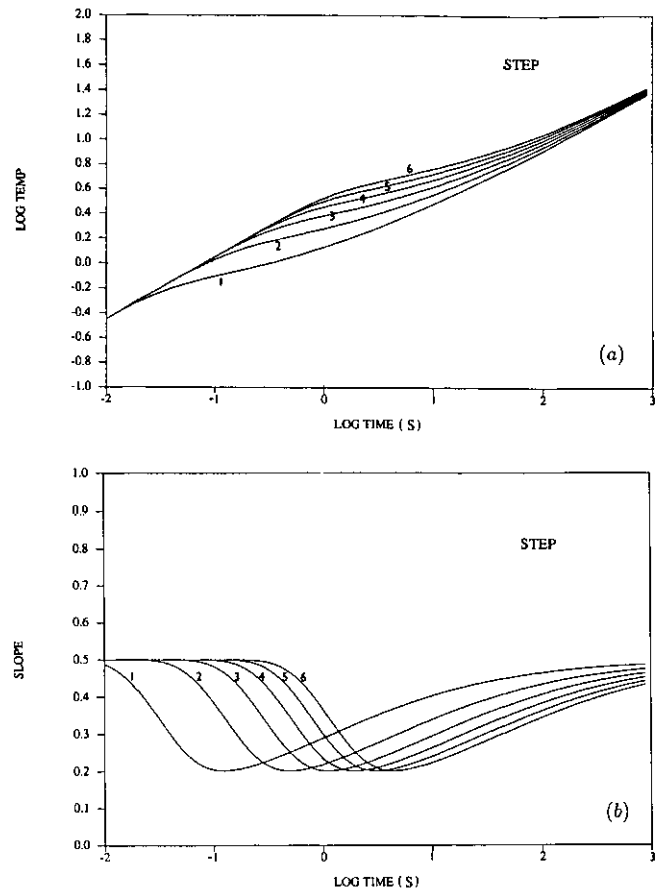


Figure 3. (a) Variation of surface temperature transients computed for step-heated opaque yttria-stabilized zirconia coatings on 316-stainless steel substrate. Heat flux $I_0 = 10000 \text{ W m}^{-2}$. Coating thicknesses are (1) 125, (2) 250, (3) 375, (4) 500, (5) 625 and (6) 750 μm . (b) Computed slope values of figure 3(a) for the stepped heating of zirconia coatings of the same thicknesses as in figure 3(a).

decay is caused by an interference effect when waves reflected from the coating-substrate interface arrive at the surface. This interference occurs at a delayed time after the absorption of the heating pulse at $t = 0$, which is proportional to the square of the coating thickness. This may be understood by referring to equation (8).

Equation (8) describes a transient thermal wave packet that propagates like a single, spreading wave crest with exponentially decreasing amplitude from the surface. This arises from thermal diffusion, which causes a spatial spreading of the temperature profile, depending on the thermal diffusivity, α , of the material. By differentiating equation (8) with respect to t and equating to zero, we obtain the time taken for the thermal wave crest to travel a distance x from the surface as [12]

$$t_{\text{peak}} = x^2/2\alpha. \quad (10)$$

The instantaneous velocity of the wave crest = $dx/dt = \alpha/x$ (or its effective velocity $x/t_{\text{peak}} = 2\alpha/x$).

Thus, the broad frequency spectrum thermal wave front initiated from the surface is seen propagating more slowly at larger distances. This is due to the

heavily damped nature of thermal waves; waves at higher frequencies propagate faster than those at lower frequency but are attenuated more, since $\mu = (2\alpha/\omega)^{1/2}$ (i.e. they are of short range propagation). The medium, in which thermal waves are propagating, acts like a 'low-pass' frequency filter characterized by its thermal diffusivity and physical dimensions.

From equation (8), we can define an effective thermal diffusion length, μ_e , similar to that of the single frequency modulated waves. In this case μ_e is the depth below the heated surface at which the temperature $T(\mu_e, t)$ is $1/e$ of the surface value $T(0, t)$:

$$\mu_e = 2(\alpha t)^{1/2}. \quad (11)$$

Similarly, when a constant heat flux of energy I_0 is applied to the surface of a semi-infinite solid for $t > 0$ (step pulse), thermal diffusion gives rise to a temperature variation within the solid ([11] p 75):

$$T(x, t) = \frac{I_0}{k} \left[(\alpha t/\pi)^{1/2} \exp\left(-\frac{x^2}{4\alpha t}\right) - \frac{x}{2} \operatorname{erfc}\left(\frac{x}{2(\alpha t)^{1/2}}\right) \right]. \quad (12)$$

The temperature at the surface ($x = 0$) of the semi-infinite solid is given by

$$T(0, t) = \frac{I_0}{k} (\alpha t/\pi)^{1/2}. \quad (13)$$

Again, an effective thermal diffusion length, $\mu_e = 2(\alpha t)^{1/2}$, can also be defined such that the temperature at $x = \mu_e$ below the heated surface is close to $1/e$ of that at the surface (at short times, the term $(\alpha t)^{1/2} \operatorname{erfc}(1)$ in the above expression for $T(\mu_e, t)$ is negligible when $x = 2(\alpha t)^{1/2}$).

At short times, the thermal diffusion length μ_e becomes small. We therefore have an initial constant slope of $+\frac{1}{2}$ in figure 3(a), which corresponds to that of equation (13) for a homogeneous semi-infinite solid.

In a coating-substrate system of different thermal properties, wave interference at the surface occurs when the effective thermal diffusion length μ_e is comparable to or greater than the coating thickness L . This condition is usually satisfied at a delayed time after the heating pulse at $t = 0$, as μ_e is a function of t (equation (11)). In fact, this time delay is, as given by equation (11), proportional to the coating thickness squared. This unique property therefore provides a valuable means of assessing the thickness or thermal diffusivity of a coating. The changes in thermal wave amplitude caused by interference, resulting in the change of shape of the curve, can be greatly enhanced by plotting the slope of the logarithmic curve ($d \log T / d \log t$) against $\log(t)$. The slopes of the computed variations of figures 2(a) and 3(a) are shown in figures 2(b) and 3(b) respectively for different coating thicknesses.

For single frequency cw excitation, the changes in phase caused by thermal wave interference at the surface are greatest when the normalized coating thickness L/μ is less than 1.5 (figure 1(b)). Therefore, we might

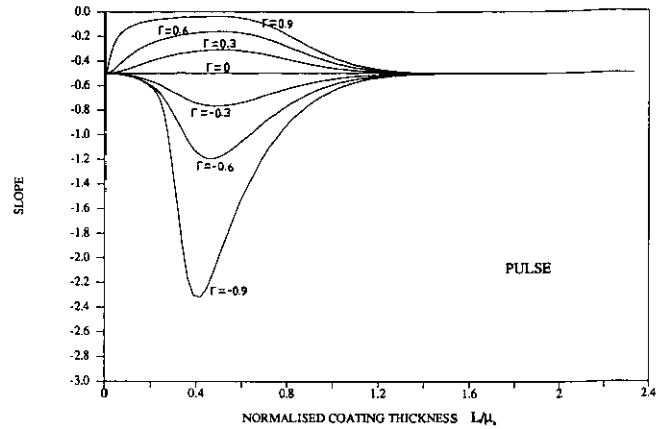


Figure 4. Variation of slope of surface temperature transients, caused by thermal wave interference, as a function of normalized coating thickness (L/μ_e) for different reflection coefficients Γ for pulsed heating.

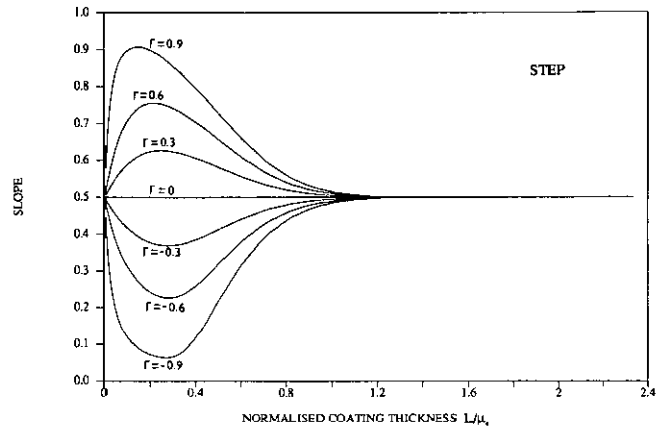


Figure 5. Variation of slope of surface temperature transients, caused by thermal wave interference, as a function of normalized coating thickness (L/μ_e) for different reflection coefficients Γ for stepped heating.

expect in the single pulse excitation that the interference effects would emerge when the normalized coating thickness L/μ_e is also less than 1.5. The rate of change of thermal wave amplitude (slope of the logarithmic thermogram), caused by interference, is shown in figures 4 and 5, plotted as a function of normalized coating thickness L/μ_e for the two pulsed modes and for different reflection coefficients. The peak interference, indicated by a minimum of the curve, occurs when the coating thickness is approximately half the effective thermal diffusion length ($L/\mu_e \sim 0.5$). Again, this is consistent with the maximum phase shift when $L/\mu \sim 0.5$ in the cw technique (figure 1(b)).

As indicated in these figures, for constructive thermal wave interference the slope values are above the $\pm \frac{1}{2}$ lines when the thermal wave reflection coefficient $\Gamma > 0$. Conversely, destructive interference occurs when $\Gamma < 0$ and is indicated by the slope values below the $\pm \frac{1}{2}$ lines. The overall magnitude of change in the

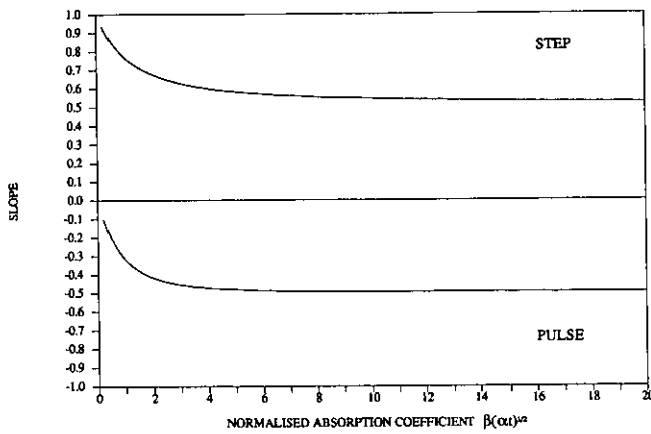


Figure 6. Deviation of slope values of surface temperature transients, caused by optical absorption effect, plotted as a function of normalized absorption coefficient $\beta(\alpha t)^{1/2}$ for a thermally thick sample.

interference region depends on the absolute value of the thermal wave reflection coefficient, which determines the amount of the thermal wave reflected to the surface from the coating-substrate interface. For a zirconia coating on steel the thermal mismatch is large, the reflection coefficient is about -0.6 , which results in the large interference effects predicted in the simulations in figures 4 and 5.

We can see immediately that although different analytical techniques are employed with periodic cw and single-pulse excitations, the characteristics of thermal wave propagation and the conditions for thermal wave interference are essentially identical. The small time shift of the interference regions between the two modes is due to the fact that the step-heating pulse has a higher energy distribution concentrated at lower frequencies; whereas the Dirac-delta pulse has an even energy distribution over a wide band of frequencies. In the periodic cw case, the energy is concentrated at a selected frequency.

It is found that for the two modes of pulsed heating there is a unique property in the temporal spacing of the logarithmic curves for different coating thicknesses. The unique spacing between different coating thickness curves is constant in all coatings, and is independent of the coating's or substrate's thermal properties. This distinctive feature seems interesting in the sense that there is a direct correspondence between coating thickness and spacing of the curves, which lends itself to coating thickness gauging. Because each thickness of a coating has its unique signature in the logarithmic curves, one can therefore, in principle, completely determine an entire coating thickness measurement in a particular coating substrate system by measuring the spacings between their logarithmic interference curves, without any knowledge of the thermal properties of the coating or substrate materials. All that is required is a single calibration measurement of a known thickness of coating for that particular system. The thermal diffusivity of the coating may be deduced from the

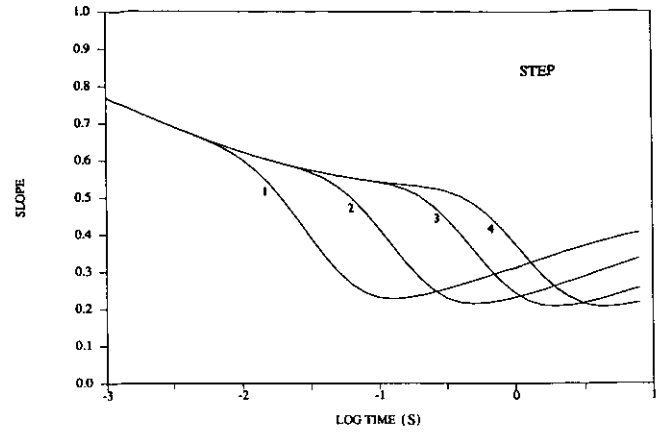


Figure 7. Effect of optical absorption on slope values for step-heated yttria-stabilized zirconia coatings on 316-steel. Coating thicknesses are (1) 125, (2) 250, (3) 500 and (4) 750 μm . The assumed absorption coefficient $\beta = 50\,000\text{ m}^{-1}$ in each case.

calibration. On the other hand, if the coating's thermal diffusivity is known, then a single measurement of the decay curve is sufficient in determining the coating thickness (equation (11)). However, if neither the coating thickness nor its thermal properties are known, we can interpret the time occurrence of the thermal interference as a measure of the coating's thermal resistance, which is an important parameter to evaluate in thermal barrier coatings.

2.2. Effect of optical absorption depth in surface coatings

The model considered above has been simplified to have the hypothetical energy deposition on the coating surface, however in some cases, such as ceramics coatings, the optical absorption effect is relatively significant over a range of coating thicknesses. This effect has been studied by a number of authors [13–15]. In photothermal excitation, the heat generated inside a sample due to the absorption of optical energy is proportional to $e^{-\beta x}$ at a distance x from the irradiated surface. The general equation of [9] is further simplified to take into account the finite optical absorption depth in a thermally thick sample:

$$T(j\omega) = \frac{I_0}{2k\sigma} \frac{\beta}{\beta + \sigma} \quad (14)$$

which reduces to, for a short pulse,

$$T(0, t) = \frac{I_0}{2k} \alpha \beta \exp(\alpha t \beta^2) \operatorname{erfc}[\beta(\alpha t)^{1/2}] \quad (15)$$

and for a step-like pulse,

$$T(0, t) = \frac{I_0}{2k} \left\{ 2(\alpha t/\pi)^{1/2} + \frac{1}{\beta} (\exp[\alpha t \beta^2] - 1) \times \operatorname{erfc}[\beta(\alpha t)^{1/2}] \right\} \quad (16)$$

Figure 6 shows the effect of sample translucency to

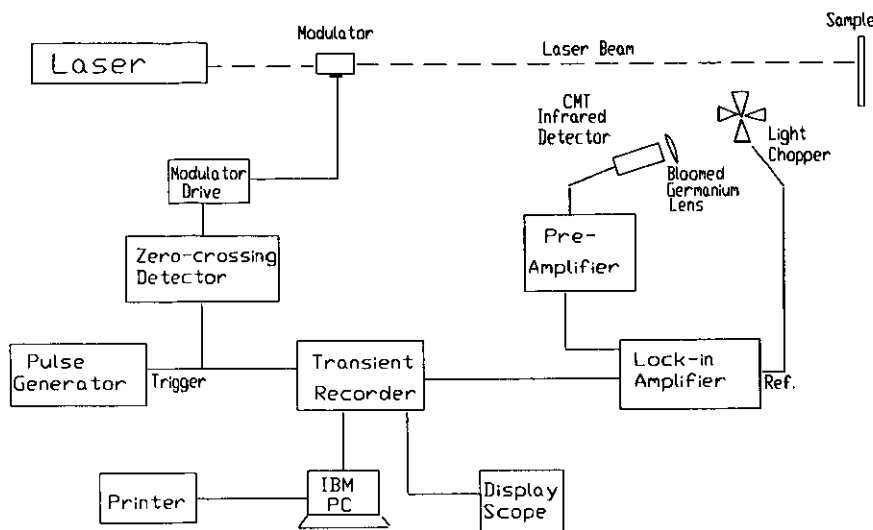


Figure 8. Schematic diagram of the experimental test system.

the excitation source on the slope values, plotted against its normalized optical absorption coefficient $\beta(\alpha t)^{1/2}$. This demonstrates that the absorption effect is only significant when $\beta(\alpha t)^{1/2} < 5$ (or when the thermal diffusion length $\mu_e = 2(\alpha t)^{1/2}$ is less than ten times the absorption depth). A simulation of the effect of step-heating an yttria-stabilized zirconia coating on steel with an optical absorption coefficient $\beta = 50\,000\text{ m}^{-1}$ for various coating thicknesses is shown in figure 7. Clearly with an equivalent absorption depth ($1/\beta$) of $20\ \mu\text{m}$, only the initial slope (+0.5 in figure 3(b)) has been significantly altered when the coating is much thicker than the absorption depth.

2.3. Advantages and disadvantages of individual thermal wave techniques

The curves in figure 2(a) show, because of the logarithmic scale, that at short times there are more significant changes in signals and a wider separation of the decay curves for thinner coatings. This is a consequence of the Dirac-delta pulse having larger number of high frequency components of short diffusion lengths, which are more suitable for resolving thinner or high diffusivity coatings. Conversely, the higher energy concentrated low frequency components of long thermal diffusion lengths of the step-heat pulse are more suitable for deep penetration in low thermal diffusivity or thick coatings. It is also well illustrated in figure 3(a), that larger signal amplitude change at long time is associated with the thicker coatings in the interference region.

It should be noted that the pulsed response can be readily obtained from a direct differentiation of the step-on heating response. The advantage of using low power step heating over high energy pulsed excitation is apparent in situations where concentrated high energy deposition may overheat and destroy the sample under inspection.

In the periodic CW approach, the frequency of the excited thermal waves can be selectively tuned, therefore a relatively low power CW laser can be used since the excitation energy is concentrated in a single frequency. In practice, the working frequency has to be carefully selected to obtain optimum thermal wave interference if measurements are carried out on a wide range of coating thicknesses. Also, for a single measurement, time has to be allowed for the transient effects to die out. On the other hand, the single-pulse transient thermal wave techniques are fast and simple to operate since a vast range of thermal wave frequencies is excited in a single shot. From a single measurement it is possible to determine a coating's thickness or its thermal diffusivity without any knowledge of the substrate's thermophysical properties. However, it requires a powerful heating source and sensitive instrumentation to capture and process the resulting thermal transients via complex computing supports.

In our experimental work, we have concentrated on the step-on heating approach as this proves to be best suited to the fairly thick plasma sprayed coatings of particular interest to us at Bath University.

3. Experimental technique

A schematic diagram of the test system is shown in figure 8. The heat source was a 5 W argon ion laser (Coherent Innova 90-5) with an unfocused beam diameter of 1 mm at its $1/e$ point. A liquid-nitrogen-cooled CMT infrared detector (Mullard J1020), coupled to a bloomed germanium lens, was used to detect the infrared emissions in the range $8\text{--}14\ \mu\text{m}$ from the excited sample surface. A lock-in detection technique was employed to reduce the noise to an acceptable level and to boost the signal output simultaneously. This incorporated the use of a lock-in amplifier (E.G.

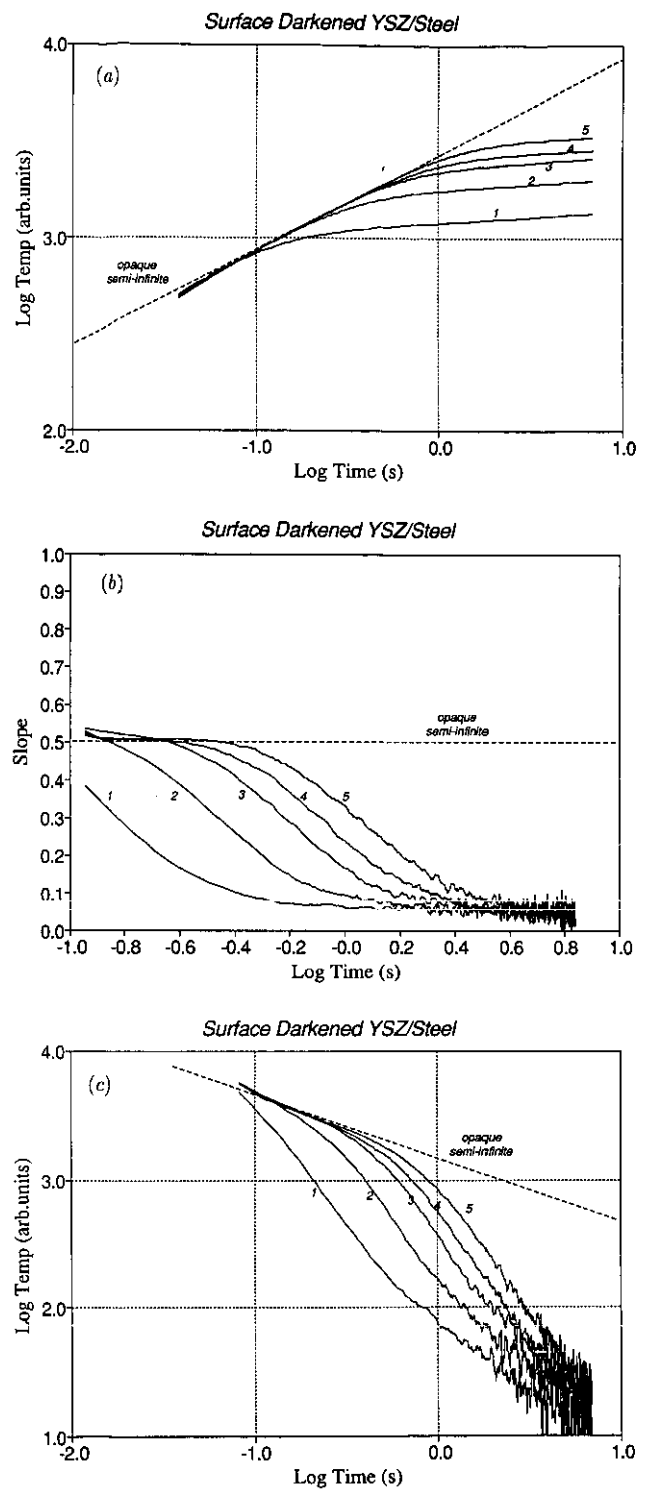
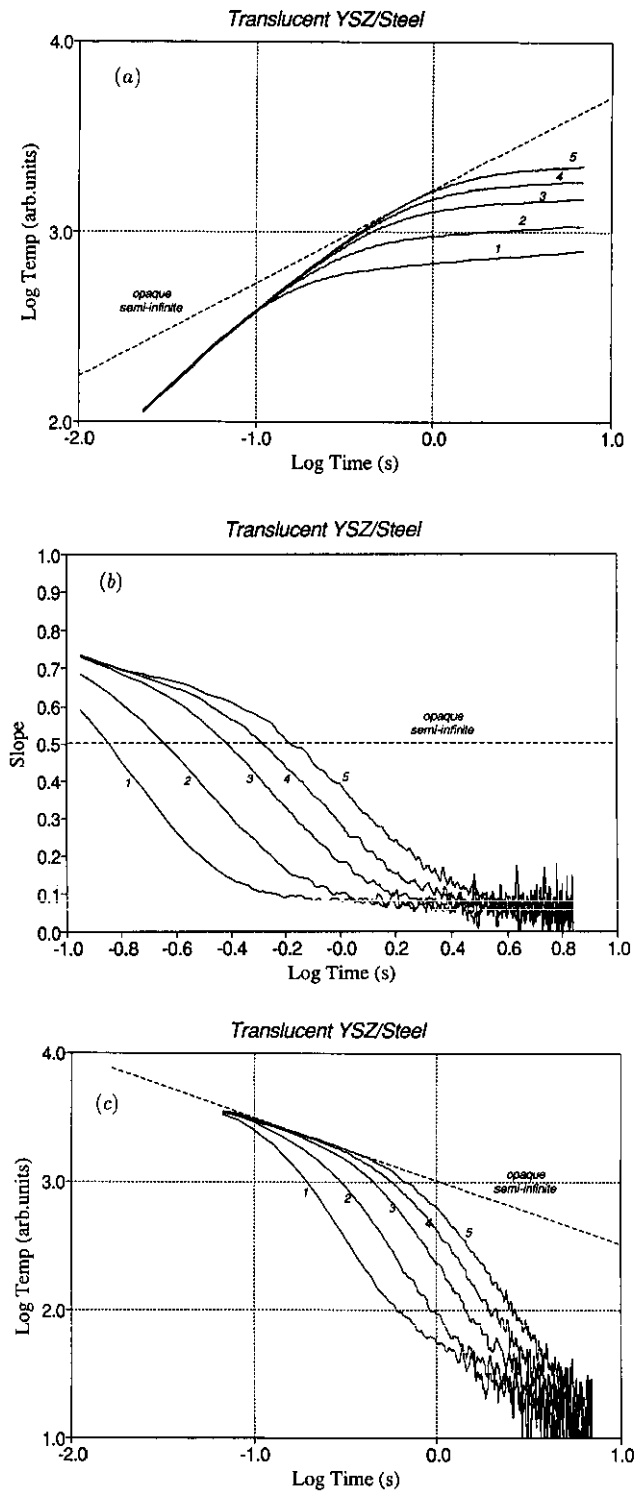


Figure 9. Experimental results obtained from step-heated normally white yttria-stabilized zirconia coatings on 2 mm thick 316-stainless steel plates. Coating thicknesses were about (1) 250, (2) 355, (3) 500, (4) 735 and (5) 850 μm . (a) Step-heating response (T against t). (b) Logarithmic slope of step-heating (a). ($(t/T)(dT/dt)$ against t .) (c) Deduced pulsed response (dT/dt against t).

Figure 10. Experimental results obtained from step-heated carbon darkened yttria-stabilized zirconia coatings on 2 mm thick 316-stainless steel plates. Coating thicknesses were about (1) 250, (2) 355, (3) 500, (4) 735 and (5) 850 μm . (a) Step-heating response (T against t). (b) Logarithmic slope of step response (a). ($(t/T)(dT/dt)$ against t .) (c) Deduced pulsed response (dT/dt against t).

& G 5206) with a mechanical light chopper (Brookdeal 9479) in front of the detector, chopping at 1 kHz to perform synchronous amplification of the detected signal. The transient analogue signals were captured and digitized directly to an IBM PC fitted with a 12-bit

programmable gain A/D converter (MetraByte DAS-8PGA) for analysis. To obtain simultaneous laser firing and transient signal recording, a positive pulse from a pulse generator was used to trigger both the transient recording and the switching of the laser acousto-optical

modulator (Acousto-Optic Modulation System 304D) via its drive electronics. It was noted that the changes in surface temperature were also determined by the optical absorption of the coating surface; marks and blemishes of the surface could significantly affect the amount of light being converted to heat. To compensate for these problems, the shape of the logarithmic plot was analysed. This was accomplished by computing the slopes of the logarithmic transient thermograms, $(t/T \times dT/dt)$.

Our main interest in this study was to find out what information could be extracted experimentally from the thermal transients. Two types of sample were prepared to test the predictions of the analysis in the preceding section: (1) Plasma-sprayed yttria-stabilized zirconia of various coating thicknesses on 2 mm thick 316-stainless steel square plates. The coating thicknesses were 250, 355, 500, 735 and 850 μm ; (2) all coatings previously inspected were locally darkened with carbon.

4. Results and discussion

4.1. Coating thickness measurement

Measurements of signal amplitude were recorded in a single-shot operation. The captured signal, $S'(t)$, was a convolution of the true transient signal, $S(t)$, with the instrumental response of the system, $h(t)$:

$$S'(t) = S(t) * h(t). \quad (17)$$

Since the response rate of a CMT infrared detector is very high, $h(t)$ is mainly governed by the lower response rate of the lock-in amplifier through its noise suppression low-pass filter circuit. The true transient signal $S(t)$ may be deconvolved using the time constant value, τ , of the lock-in amplifier by

$$S(t) = S'(t) + \tau \frac{dS'(t)}{dt}. \quad (18)$$

Figure 9(a) shows the logarithmic temperature plots of the processed experimental data from the five different coating thickness measurements of the normal white zirconia coatings. Figure 9(b) corresponds to the logarithmic slopes of the curves in figure 9(a). Figure 9(c) shows the deduced pulsed response of figure 9(a) by taking its time derivatives. All these measurements were obtained using 3.5 W laser power and 10 ms lock-in time constant. During each temperature measurement, the sensitivity of the lock-in amplifier was adjusted to maximize the resolution of the A/D converter. The results of the temperature plots shown in figures 9(a) and (c) were therefore scaled accordingly so that their initial portions matched one another. Repeated measurements showed that these curves were reproducible. It is evident that the temporal separation of these curves corresponds directly to the thickness of the coating; and the curves of the thin coatings inflect, as predicted, from the initial linear rise much earlier than those of the thicker coatings.

The initial portion of these curves up to about the inflection region is consistent with the one-dimensional theoretical predictions, using the literature values of thermal properties for zirconia coating and 316-steel substrate previously listed. The curves do, however, illustrate the inadequacy of the one-dimensional thermal wave model at long times. Results from a finite-difference numerical analysis on a finite spot size of laser heating [6] show that this arises from the effects of three-dimensional signal saturation toward the end of the thermogram. At long times, when the surface temperature builds up, other physical effects can occur, such as convection and radiation, that have not been taken into account. This alters the thermal wave interference (a 'trough' in the 1D case), making the determination of the coating thickness rather uncertain.

The effect of coating translucency, as studied above, has a significant influence on the initial part of the thermal response. Of all the curves examined in figures 9(a) and (b), deviations of the initial constant slope of $+\frac{1}{2}$ for the opaque case are mainly attributed to this translucent effect. To demonstrate its significance, the samples were subsequently darkened by rubbing a piece of carbon over their surfaces. Figure 10(a) shows the results of the logarithmic temperature plots of the five darkened zirconia samples, and figure 10(c) the deduced pulsed response. The effect of carbon darkening caused a noticeable increase in both the optical absorption and infrared emissivity of the surface. The increase in signal-to-noise ratio is highlighted by plotting its logarithmic slope in figure 10(b). The darkening of coating surface appears to have significantly reduced the optical penetration in the coating, as the initial slope is closer to that of an opaque one. The inflection points (the starting points of thermal wave interference) are now more clearly defined than those observed in the optically translucent coatings in figure 9(b), and are in good agreement with the theoretical prediction. This further suggests that the position of the inflection point may provide a useful means of gauging coating thicknesses. Unfortunately, the low signal-to-noise ratio of the initial transient response may sometimes obscure the required features at short times, making the determination of inflection points for the thinner coatings particularly uncertain.

5. Conclusions

The experimental results have clearly demonstrated that the transient thermal wave technique described here is suitable for testing coatings of plasma-sprayed zirconia on stainless steel. The technique is attractive because it is non-destructive, non-contacting and operated in a single shot mode. Examination of the analysis of the optically translucent model and the experimental results have exposed the significance of the translucency of zirconia coatings. This can sometimes obscure the determination of the inflection point and

the interpretation of the required features of the thermal response. If care is taken to minimize such effects and if the measurement time is short, the simple one-dimensional opaque model is adequate. The investigation of the two theoretical models (optically opaque and translucent) and the experimental results has further revealed that although the logarithmic spacing of the thermal response curves gives a good indication of the coating thickness variations, the precise relationship is modified by the translucency of a particular coating. The position of the inflection point, which is a measure of the time taken for the thermal wave front returning from the interface to the coating surface, is a more reliable parameter for gauging coating thickness. This appears to be less affected by the optical penetration and three-dimensional heat spread effects if the former is small compared with the coating thickness. Unfortunately, as mentioned earlier, the low signal-to-noise ratio impairs the detection of low amplitude signal at short times.

References

- [1] Almond D P, Patel P M, Pickup I M and Reiter H 1985 *NDT Int.* **18** (1) 17
- [2] Patel P M and Almond D P 1985 *J. Mater. Sci.* **20** 955
- [3] Patel P M, Almond D P and Reiter H 1987 *Appl. Phys.* **B** 43 9
- [4] Tam A C and Sontag H 1986 *Appl. Phys. Lett.* **49** 1761
- [5] Cielo P 1984 *J. Appl. Phys.* **56** 230
- [6] Cielo P and Dallaire S 1985 *ASM Metals Congress (Toronto, Canada)* p 166
- [7] Cielo P, Lewak R, Maldague X and Lamontagne M 1986 *C.S.N.D.T. Journal* **7** 2
- [8] Frederikse H P R and Ying X T 1988 *Appl. Opt.* **27** 4672
- [9] Bennett C A and Patty R R 1982 *Appl. Opt.* **21** 49
- [10] Parker W J, Jenkins R J, Butler C P and Abbott G L 1961 *J. Appl. Phys.* **32** 1679
- [11] Carslaw H S and Jaeger J C 1959 *Conduction of Heat in Solids* (Oxford: Clarendon Press)
- [12] Kanstad S O and Nordal P E 1986 *Can. J. Phys.* **64** 1155
- [13] Tam A C and Sullivan B 1983 *Appl. Phys. Lett.* **43** 333
- [14] Imhof R E, Birch D J S, Thornley F R, Gilchrist J R and Strivens T A 1984 *J. Phys. E: Sci. Instrum.* **17** 521
- [15] Tischler M, Kohanoff J J, Rangugni G A and Ondracek G 1988 *J. Appl. Phys.* **63** 1259